

New Insight Into Intestinal Motor Function via Noninvasive Endoluminal Image Analysis

CAROLINA MALAGELADA,* FOSCA DE IORIO,* FERNANDO AZPIROZ,* ANNA ACCARINO,* SANTI SEGUI,[‡] PETIA RADEVA,[‡] and JUAN-R. MALAGELADA*

*Digestive System Research Unit, University Hospital Vall d'Hebron; Centro de Investigación Biomédica en Red de Enfermedades Hepáticas y Digestivas (Ciberehd); Department of Medicine, Autonomous University of Barcelona, Barcelona, Spain; and [‡]Computer Vision Center, Bellaterra, Spain

Background & Aims: Evaluation of small bowel motility by intestinal manometry is invasive and requires expertise for interpretation. Our aim was to use capsule technology for evaluation of small bowel motor function based on a fully computerized image analysis program. **Methods:** Thirty-six consecutive patients with severe intestinal motor disorders (19 fulfilling manometric criteria of intestinal dysmotility and 17 not) and 50 healthy subjects received the endoscopic capsule (Pillcam; Given Imaging, Yokneam, Israel). Endoluminal image analysis was performed with a computer vision program specifically developed for the detection of contractile patterns (phasic luminal closure and radial wrinkles by wall texture analysis), noncontractile patterns (tunnel and wall appearance by Laplacian filtering), intestinal content (by color decomposition analysis), and endoluminal motion (by chromatic stability). Automatic classification of normal and abnormal intestinal motility was performed by means of a machine-learning technique. **Results:** As compared with healthy subjects, patients exhibited less contractile activity (25% less phasic luminal closures, $P < .05$) and more noncontractile patterns (151% more tunnel pattern, $P < .05$), static sequences (56% more static images, $P < .01$), and turbid intestinal content (94% more static turbid images, $P < .01$). On cross validation, the classifier identified as abnormal all but 1 patient with manometric criteria of dysmotility and as normal all healthy subjects. Out of the 17 patients without manometric criteria of dysmotility, 11 were identified as abnormal and 6 as normal. **Conclusions:** Our study shows that endoluminal image analysis, by means of computer vision and machine-learning techniques, constitutes a reliable, noninvasive, and automated diagnostic test of intestinal motor disorders.

Small bowel motor dysfunction may cause severe clinical syndromes, such as intestinal pseudoobstruction, reduced tolerance to feeding, and inability to maintain normal body weight. The current gold standard for the evaluation of small bowel motor function is intestinal manometry.^{1,2} However, the application of this technique

has been restricted to few referral centers owing to the complex technical procedure and the expertise demanded in the interpretation of results. Furthermore, manometry is an invasive diagnostic method that entails some degree of discomfort for the patient.

Recently, the technology of capsule endoscopy has been developed.³ The PillCam (Pillcam SB video capsule; Given Imaging, Yokneam, Israel) capsule transmits endoluminal images every half second to an external receptor over 8 hours. As opposed to manometry, which only detects the pressure changes produced by occlusive phasic contractions, endoluminal imaging provides continuous visualization of the intestinal walls, lumen, and content and permits detection of contractile events (both complete and incomplete luminal occlusions), as well as noncontractile patterns (open tunnel and smooth wall patterns), type of contents (chyme, secretions), and movement of parietal and endoluminal structures.

We hypothesized that small bowel motor function can be quantitatively evaluated by endoluminal image analysis; consequently, our aim was to develop a noninvasive, simple procedure for automatic identification of intestinal motor dysfunction. To this end, we applied advanced computer vision technology. Using a multidisciplinary team approach, we created a series of tools, ie, algorithms, for computer analysis of various endoluminal features. Fine-tuning of computer vision analysis was implemented by multiple-step visual feedback of the computer algorithm output. To prove its clinical validity, the discriminatory power of this technology was then tested against manometry in a group of patients with clinical symptoms suggestive of severe intestinal motor dysfunction.⁴

Patients and Methods

Participants

A series of 36 consecutive patients (10 men, 26 women; age range, 18–78 years) referred for evaluation of severe symptoms suggestive of small bowel motor dys-

Table 1. Manometric Criteria of Abnormal Motility

- A. Abnormal configuration of interdigestive phase III: Tonic rises of baseline pressure over 30-mm Hg amplitude \geq 3-minute duration.
- B. Abnormal propagation of interdigestive phase III: Simultaneous or retrograde propagation over \geq 20-cm intestinal segment.
- C. Absence of normal fed pattern: No changes in activity during postprandial period (no fed pattern) or phase III-like activity during postprandial period (while disregarding the first 20 minutes after beginning of meal).
- D. Bursts: At least one period of \geq 5 minutes or 2 periods of \geq 2-minute duration with continuous high amplitude (\geq 20 mm Hg) and high-frequency (10–12/min) phasic pressure activity not followed by motor quiescence.
- E. Sustained contractions: Prolonged (\geq 30 minutes duration), high-amplitude (\geq 20 mm Hg) and high-frequency (10/min) phasic pressure activity at an intestinal segment with normal or reduced activity recorded at other levels.
- F. Hypomotility: Low-amplitude contractions (no contractions $>$ 10 mm Hg).

NOTE. Based on these criteria, 16 manometric tracings were classified as neuropathic-type pattern (at least one criterion from A to E), 3 as myopathic-like pattern (generalized hypomotility), and 17 did not fulfill criteria of abnormality.

function and 50 healthy subjects (23 men, 27 women; age range, 18–36 years) without gastrointestinal symptoms were included in the study. After mechanical intestinal obstruction and gut lesions had been ruled out by a thorough workup, all patients underwent conventional small bowel manometry. In this pilot study, no formal sample size calculations could be performed, and the total number of participants (patients plus healthy subjects) was estimated based on the number of parameters included in the diagnostic algorithm (see below).

Patients presented either (1) relapsing acute episodes of intestinal pseudoobstruction with radiologic evidence of intestinal air-fluid levels ([mean \pm SE] 2.8 ± 1.7 episodes per year) interspersed with relatively symptom-free intervals ($n = 16$), (2) chronic abdominal symptoms and distention resembling partial mechanical obstruction of the gut ($n = 2$), or (3) postprandial symptoms (nausea, vomiting, abdominal discomfort/pain, bloating) with reduced feeding tolerance and inability to maintain

normal body weight, ie, body mass index below 18.7 in women and 20.1 in men ($n = 18$).

Small bowel manometry was performed using a standard technique, as previously described.⁴ Briefly, after an overnight fast, a manometric tube (9012X1106 Special Manometric Catheter; Medtronic, Skovlunde, Denmark) was orally introduced into the jejunum under endoscopic guidance. Five manometric ports spanned at 10-cm intervals were positioned from the proximal duodenum to the midjejunum under fluoroscopic control. Stationary recording was performed for 3 hours during fasting and 2 hours after ingestion of a solid-liquid meal (450 kcal). Manometric diagnosis of abnormal motility was established using the criteria routinely used in our unit (Table 1) that are based on previously published data.^{4,5} Nineteen patients fulfilled these manometric criteria of intestinal dysmotility and 17 did not (Table 2). The protocol for the study was approved by the Ethics Committee of the University Hospital Vall d'Hebron, and all participants gave their written informed consent.

Endoluminal Imaging

The PillCam capsule (Given Imaging) was used to visualize the intestinal lumen at a twice per second rate. Six external antennae were fixed to the anterior abdominal wall to register intraluminal images transmitted from the capsule. The battery in the capsule permitted a total recording time of 8 hours.

Test Procedure

The same preparatory procedures were observed as for conventional intestinal manometry, eg, no medications that could affect gastrointestinal motility, overnight fast, and, in the case of gastric retention of food residues, nasogastric suction and/or prolonged ($>$ 24 hours) fasting. It should be noted that, in patients with recurrent episodes of acute intestinal pseudoobstruction, evaluation of intestinal motility, either by manometry or capsule endoscopy, was performed during periods of clinical remission.

After ingestion, gastric exit of the capsule was monitored by endoluminal visualization (intestinal mucosa

Table 2. Clinical and Manometric Data

Clinical data	Manometric criteria of abnormality			Subtotal
	Neuropathic	Myopathic	No criteria	
Acute pseudoobstruction	7 (+)	0	6 (+)/1 (–) ^a	14
Chronic pseudoobstruction	0	0	2 (+)	2
Food intolerance	9 (+)	3 (+)	5 (+)/3 (–)	20
Subtotal	16	3	17	

NOTE. Data are number of patients classified as normal (–) or abnormal (+) by endoluminal image analysis.

^aAmong these 7 patients, 1 patient had a single burst $<$ 5 minutes duration, 4 patients (3 abnormal by endoluminal image analysis; 1 normal) exhibited a minute rhythm pattern (defined as regular bursts of 30–60 seconds every 1–3 minutes during \geq 30 minutes of the postprandial period without demonstrable luminal compromise), and 2 patients had normal manometry (1 later diagnosed of intestinal myopathy and the other of neuropathy by full-thickness biopsy).

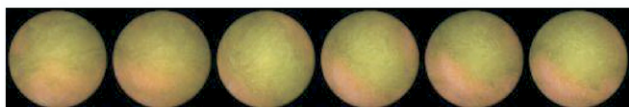
pattern) at 10-minute intervals using a real-time viewer monitor (RAPIDAccess; Given Imaging). Sixty minutes later, participants were asked to ingest a liquid meal (Ensure HN; Abbott, Zwolle, The Netherlands; 300 mL, 1 kcal/mL). The study was continued for a total recording time of 8 hours with the subjects lying comfortably on a hospital bed with the trunk 30° above the horizontal. In a series of preliminary feasibility studies, the optimal characteristics of the meal for inducing a potent and consistent motor response without impairing endoluminal vision were determined.⁶ Furthermore, with the capsule fixed to an endoluminal tube, we also established that the depth of view of endoluminal images was 1–3 cm, and the image patterns were similar with either antegrade or retrograde vision. All studies were first analyzed visually to rule out intestinal lesions.

Analysis of Specific Patterns

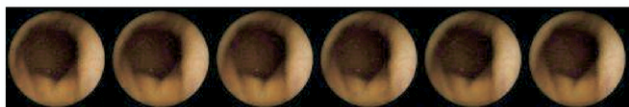
Gastric exit of the capsule and arrival in the cecum were visually detected, and small bowel images were analyzed. Endoluminal image analysis was performed by means of a computer vision program specifically developed for the evaluation of intestinal motility. Tools for analysis were developed and are sequentially detailed below.

Turbid content. Gas or liquid intestinal content, usually transparent, permits a nitid, clear view of the intestinal walls and lumen. However, some images are

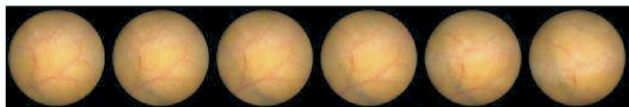
Turbid content



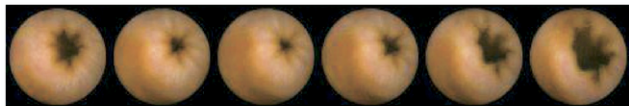
Tunnel pattern



Wall pattern



Occlusive contraction



Non-occlusive contraction

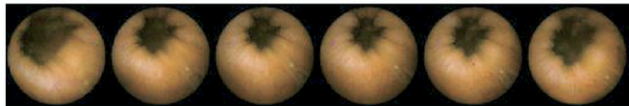


Figure 1. Endoluminal image patterns. Examples of 6-frame sequences. Note phasic luminal closure and radial wrinkles in occlusive and nonocclusive contractions.

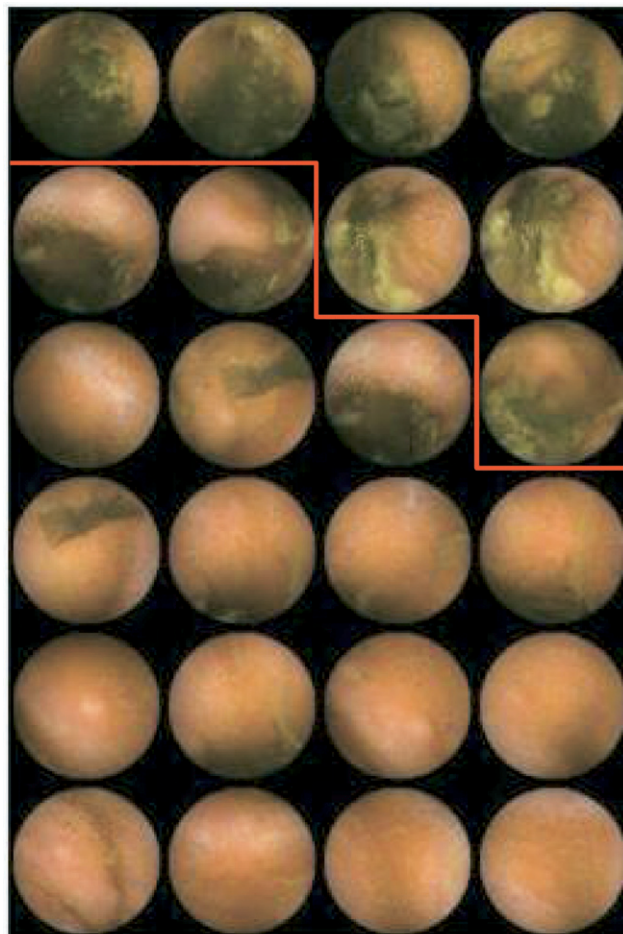


Figure 2. Example of a study visualized as a self-organizing map for turbid frame classification. Similar images are grouped together to permit a semisupervised classification.

blurred by turbid intestinal content (Figure 1). Turbid images were detected by color analysis using the opponent color decomposition technique.⁷ Each image was defined by 2 parameters representing the mean value (chromacity) of the blue-yellow vs the red-green component. Visualization of all the images, ie, frames, from a study was simplified by self-organizing maps (Figure 2): similar images are grouped together, and representative images of each group are then displayed in 2 dimensions ordered by similarity, similar groups in vicinity and the distance reflecting dissimilarity.⁸ Using this representation, turbid images were selected using a semisupervised approach: the investigator selected clear examples of turbid and nonturbid (clear) images, and the computer algorithm, using these examples as a training set, completed the classification (turbid/nonturbid) of all the images in the video.

Tunnel and wall patterns. In each image, the relationship between the intestinal walls and lumen was analyzed as follows. Images were first converted into a gray scale, and the intensity of light of the different pixels in the image was analyzed using a Laplacian of Gaussian

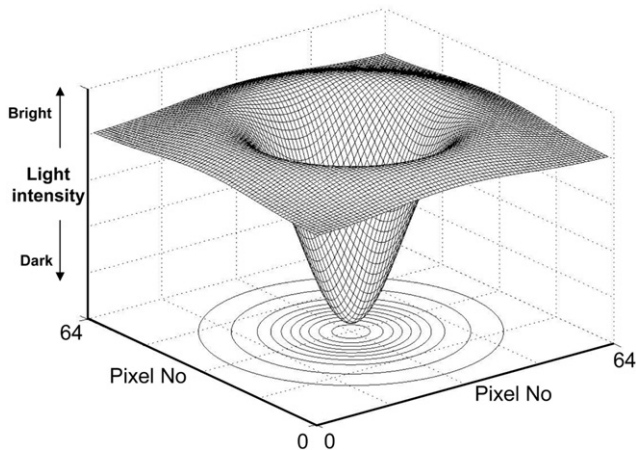


Figure 3. Laplacian of Gaussian model. The intensity of light of the pixels in each image was analyzed using a 3-dimensional curve that reflects the relationship between the bright walls close to the light of the capsule and the dark lumen.

model (second-order symmetry filter with a training parameter delta fixed at 3), which defines the 3-dimensional curve (Figure 3) reflecting the relationship between the bright walls close to the light of the capsule and the dark lumen.⁹ A tunnel pattern (open lumen) was visualized as a band of bright peripheral wall and a central lumen characterized by a large dark area. A frame was then labeled as tunnel (Figure 1) when the mean lumen area of the 9 neighbors (4 frames before and 4 after) was above a certain threshold. A tunnel sequence was defined as 60 or more consecutive frames with a tunnel pattern permitting gaps of 5 or fewer nontunnel frames. Conversely, a wall pattern, reflecting a transverse endoluminal view (Figure 1), was characterized by an image directly focusing on a smooth bright wall without a view of the lumen.

Static images. Visualization of the sequence of images in the video reflects endoluminal movement depending on the dissimilarity of sequential frames. Static sequences were detected by analysis of color differences in consecutive images using the Earth Mover's Distance method¹⁰ as follows. The color distribution of each frame is measured in a 64-color plot depending on the red-green-blue composition. The method measures the minimal amount of work (Euclidian distance) necessary to transform the plot corresponding to one frame into the following one. A preliminary validation study was performed in 6 subjects, each of whom received an intravenous infusion of glucagon (4.8- $\mu\text{g}/\text{kg}$ bolus followed by 9.6 $\mu\text{g}/\text{kg}/\text{h}$ for 1 hour) to determine the parameters reflecting lack of endoluminal movement (static images).¹¹ This dose of glucagon has been previously shown to produce complete inhibition of both tonic and phasic intestinal motor activity.^{12,13} A frame was considered static when the mean Euclidian distance between 40 consecutive neighbors was below a certain threshold

(0.01). A static sequence was then defined as 60 or more consecutive static frames permitting a gap of 10 or fewer nonstatic frames.

Phasic luminal closure. Phasic intestinal contractions (Figure 1) are visualized as reversible changes in lumen size (closure/opening) within a 9-frame sequence (4.5 seconds). These events were detected using a cascade of sequential steps.¹⁴ In the first step, the images blurred by turbid contents were automatically filtered out using the turbid detection algorithm described above. In the second step, images corresponding to static sequences were automatically rejected using the static image filter described above. After having reduced the number of candidate sequences by this pretreatment, the third step in the cascade applied a discrimination algorithm (classifier) based on a machine-learning technique (support vector machine).¹⁵ From the Laplacian analysis of each image described above (see tunnel and wall pattern), 54 parameters were measured in each 9-frame sequence. Based on a series of examples of contraction sequences ($n = 11,046$) and noncontraction sequences ($n = 44,361$) selected by visual analysis, the machine found the best discriminatory function to classify contractions as reversible lumen closure.

Luminal closure during intestinal contractions may be complete (occlusive contractions) or not (Figure 1). Discrimination between occlusive and nonocclusive contractions was performed by a second classifier (support vector machine) based on a training set of both types of contractions ($n = 768$) identified by visual analysis.

Radial wrinkles. Contraction of the circular intestinal muscle produces wrinkles in the intestinal wall radial to the shrinking intestinal lumen (Figure 1). In each image, the amount of intestinal wrinkles was measured by structural tensor analysis^{16,17} as follows. The image was treated as a topographic map in which the crests and valleys were identified and skeletonized. The height of the crests and their direction toward the central lumen were measured to determine their global directional energy (entropy). Using a radial Gaussian basis function kernel with delta set at 4, the degree of wrinkles was measured from 0 to 1.

Statistical Analysis

Mean (or grand mean) values ($\pm\text{SE}$) of the parameters measured were calculated in each group of subjects. The normal range of each parameter was established as the 5th–95th percentile of the values in healthy subjects. Comparisons of individual parameters between different groups (healthy subjects vs patients; male vs female; older half vs younger half) were made by unpaired Student *t* test for parametric, normally distributed data; otherwise, the Mann–Whitney *U* test was used. Frequency analysis was performed by the χ^2 test.

Algorithm for Discrimination Between Patients and Healthy Subjects

Discrimination between the 2 groups was performed using a machine-learning technique (support vector machine)¹⁵ as follows. From the features analyzed, 42 parameters were measured; hence, each subject was defined by 42 dimensions. Given a series of examples, as a training set, the program draws the hyperplane that separates in a multidimensional space patients from healthy subjects with the maximum margin between them (Figure 4). In essence, based on the data of the training set, the program first learns to identify the differences and, instead of defining cutoffs for each individual parameter, finds the combinations of parameters that best discriminate both groups and constructs the function that defines the separating plane. The group of patients with manometric criteria of dysmotility and the group of healthy subjects were used as the initial training set. With the resulting function, the patients not fulfilling manometric criteria of dysmotility were then tested, and those

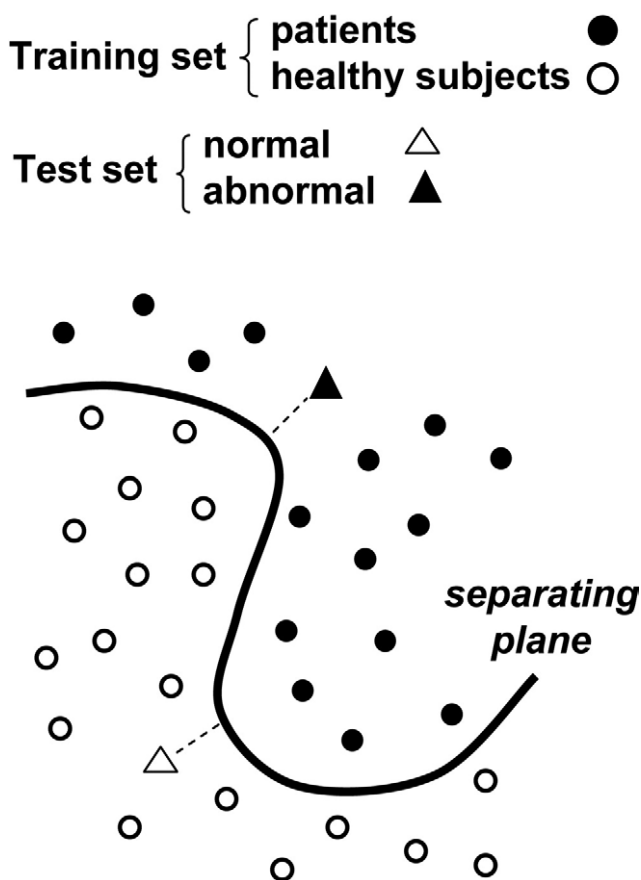


Figure 4. Discrimination of patients by a machine-learning technique. Each subject is defined by 19 parameters; based on a training set, the program first learns to identify the differences (combination of parameters) between healthy subjects (normal) and patients (abnormal) and draws the separating plane with maximum margin between them. Any new case (test set) is then classified as normal or abnormal, and its distance to the separating plane reflects the certainty of the diagnosis.

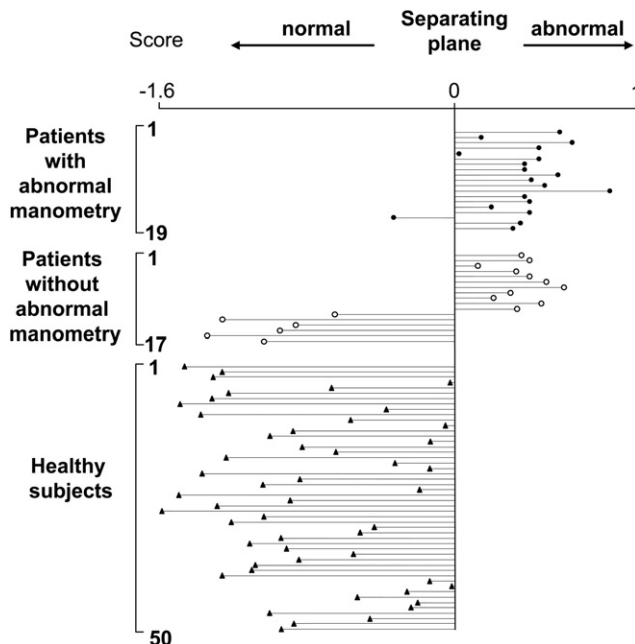


Figure 5. Cross validation of the classification algorithm. Each subject was sequentially tested using the remainder (all but himself) as the training set. Note that, on cross validation, all subjects, except 1 patient with abnormal manometry, were correctly classified.

identified as abnormal by the program were used to expand the training set and thereby enhance the stability of the algorithm.¹⁸

Cross validation of the algorithm was performed by partitioning the data sample into 2 subsets: one was used for training (training set), and the other was then tested (validation or testing set). From the various methods of cross validation, we selected the leave-one-out method¹⁹: one subject from the original data sample is retained as the testing set and the remainder (all but himself) as the training set; the procedure is repeated for all subjects, and the distance of each subject to the separating plane reflects the certainty of the diagnosis (Figure 5). This method was also applied to reduce the number of parameters included in the algorithm to the minimum number that still preserved the discriminatory power of the function. Nineteen of the 42 parameters initially tested were found to have discriminative value in the classifier (Table 3). Because the discriminatory power of the support vector machine was not further improved by introducing additional parameters, these 19 discriminating parameters were retained for use in the classifier.

Results

Healthy Subjects

In 34 subjects, the capsule reached the colon, and mean transit time from the duodenum to the cecum was 206 ± 11 minutes. Turbid content was detected $27\% \pm 2\%$ of the time. Endoluminal images reflected a wall pattern $22\% \pm 1\%$ of the time and an open tunnel pattern

Table 3. Parameters Used in the Classifier to Discriminate Patients and Healthy Subjects

Parameters	Normal range	
	5th–95th percentile	Patients ^a outside normal range
Turbid frames (%)	8.9–59.1	11
Tunnel in nonturbid frames (%)	0.1–21.1	5
Duration of tunnel sequences, seconds (s)	0.0–99.1	3
Total static frames (%)	4.0–41.7	8
Nonturbid static frames (%)	4.3–43.8	6
Turbid static frames (%)	1.6–36.0	10
Nonturbid frames, static degree ^b	0.01–0.02	6
Turbid frames, static degree ^b	0.01–0.03	7
Tunnel sequences, static degree ^b	0.01–0.05	1
Duration of static sequences (s)	18.6–84.3	5
Frames with wrinkles (>0.7 degrees) (%)	2.8–13.4	10
Duration of wrinkle sequences (s)	3.4–7.7	8
Nonturbid frames with wrinkles (%)	2.8–13.2	10
Frames with low degree of wrinkles (<0.1) (%)	56.4–82.5	8
Frames with high degree of wrinkles (>0.9) (%)	1.1–7.9	9
Phasic luminal closures		
Events per min	2.4–6.1	10
Events per min in nonturbid images	3.7–7.7	12
Nonocclusive events (%)	0.2–11.2	8
Events with wrinkles (in at least 1 of the 5 central frames) (%)	15.3–52.5	5

^aPatients with manometric criteria of abdominal intestinal motility (n = 19).

^bStatic degree measured by the Earth Mover's Distance method.

4% ± 1% of the time. A tunnel pattern appeared in 28 ± 5-second sequences. During the studies, 925 ± 53 events of phasic luminal closure were detected (4.0 ± 0.2 events per minute), in 3.2% ± 0.4% of which luminal closure was incomplete (nonocclusive contractions). A high degree of wrinkles (>0.7) was detected in 4.1% ± 0.3% of frames. In the videos, 24% ± 1% of the images were static, ie, corresponded to static sequences. The mean duration of static sequences was 42 ± 3 seconds. The image was static in 18% ± 2% of frames showing turbid intestinal content, 10% ± 3% of those showing a tunnel pattern, and 34% ± 2% of those showing a wall pattern. No age and sex differences were detected.

Patients With Manometric Criteria of Intestinal Dysmotility

The capsule reached the cecum in only 5 patients, and in them small bowel transit time was 248 ± 38 minutes. Patients had more turbid content in the gut than healthy subjects (37% ± 7%, respectively), and 11 were outside the normal range. Furthermore, in contrast to healthy subjects, turbid content in patients was frequently static (35% ± 5% static turbid content, $P = .005$ vs healthy subjects). Wall pattern images were less frequent in patients (12% ± 2%) than in healthy subjects

($P = .0001$). By contrast, the tunnel pattern was more frequently seen in patients (11% ± 2% of the time, $P = .01$ vs healthy subjects), and tunnel sequences (59 ± 12 seconds) were longer than in healthy subjects ($P = .008$). Another distinctive feature in patients was a reduced number of phasic luminal closures (3.0 ± 0.6 events per minute, $P = .012$ vs healthy subjects), and, furthermore, a greater proportion of them were incomplete (8.4% ± 1.9% nonocclusive contractions, $P = .014$ vs healthy subjects). Overall, a high degree of wrinkles (>0.7) was detected in a similar proportion to healthy subjects (5.0% ± 1.1% of the frames); however, the individual distribution differed, and 9 patients were outside the normal range. The intestine appeared more static in patients (38% ± 4% static images, $P = .006$ vs healthy subjects), and this applied to frames showing turbid content (see above) and also to nonturbid images (38% ± 5% were static, $P = .027$ vs healthy subjects). Furthermore, static sequences (73 ± 12 seconds) were more prolonged than in healthy subjects ($P = .002$). No age differences were detected.

Out of the 19 parameters found to have discriminative value in the classifier (Table 3), patients with abnormal manometry showed a mean of 7.5 ± 1.0 parameters outside the normal range ($P < .0001$ vs 1.5 ± 0.3 in healthy subjects). In 15 of the 19 patients (84%), but only 6 of the 50 healthy subjects (16%), more than 2 parameters were outside the normal range ($P < .0001$).

As compared with the 16 patients with neuropathic type dysmotility, the 3 patients with myopathic-like dysmotility pattern had more turbid content (76% ± 21% vs 30% ± 7% of the images, respectively; $P = .025$), less wrinkles (0.7% ± 0.2% vs 6.0% ± 1.1%, respectively; $P = .04$), and less phasic luminal closures (0.5 ± 0.3 vs 3.5 ± 0.6 events per minute, respectively; $P = .034$).

Discrimination Between Patients and Healthy Subjects by Machine-Learning Technique

The classifier identified as abnormal all patients with manometric criteria of dysmotility and as normal all healthy subjects. Eleven of the 17 patients without manometric criteria of dysmotility were identified as abnormal and 6 as normal.

Among the 30 patients identified as abnormal by endoluminal image analysis, no distinctive features were detected when comparing subgroups of patients with different clinical presentation (pseudoobstruction vs reduced feeding tolerance). However, in this group, patients with abnormal manometric criteria (n = 19), as compared with those without (n = 11), had more static images (38% ± 5% vs 21% ± 3%, respectively; $P < .006$) and less phasic luminal closures (4.1 ± 0.6 vs 6.3 ± 0.7 events per minute, respectively; $P = .032$). No differences were detected between patients found normal by endoluminal image analysis and healthy subjects.

Cross validation using the leave-one-out method evidenced a very high sensitivity and specificity of the algo-

rhythm. All healthy subjects were correctly classified. Only one patient with abnormal manometry was missed in the cross validation. Among the patients without manometric criteria of dysmotility, both subgroups identified as normal and as abnormal were correctly classified (Figure 5).

Discussion

This study shows that endoluminal image analysis by means of computer vision and machine-learning techniques constitutes a reliable, noninvasive, and automated diagnostic test of intestinal motor disorders. The conceptual and methodologic development presented here represents the outcome of a 5-year multidisciplinary project on computer processing of information acquired by capsule endoscopy. The fundamental hypothesis of this research was that many physiologically relevant events remain undetected by intestinal manometry that only registers punctual pressure changes produced by occlusive contractions. As the immediate hypothesis, we postulated that these events detected by capsule endoscopy can be used for small bowel motility evaluation.

Computer vision has been developed in recent decades with a variety of applications, such as face recognition, fingerprint identification, topographic analysis of terrestrial surface, and texture analysis of materials. The first step in the procedure is to measure certain aspects, or features, related to the light intensity or color composition of the image by applying specific mathematic models. Once these features have been translated into numeric parameters, they are analyzed to determine whether they adjust to a specific pattern. Automated classification of data is performed by machine-learning techniques. Based on a series of examples provided as a training set, different algorithms can be applied. These algorithms weigh the discriminatory power of the parameters analyzed and find the function that best discriminates between positive and negative examples. Any new case, or test set, defined by the same type of parameters, can then be automatically classified. Development of computer vision programs requires multiple trial-and-error loops using visual feedback to determine whether the computer output truly reflects what the human eye detects (visual pattern recognition) and tune the feature extraction and analysis algorithms accordingly.

Endoluminal images were acquired by means of an endoscopic capsule with a transparent front and a photographic camera and illumination system within. In the unprepared, noninsufflated gut, the existence of gas or transparent liquid content generally permits a clear view of the intestinal walls and lumen analogous to conventional or subaquatic photography. The capsule advances propelled by peristaltic activity and simultaneously registers the contractile activity it "sees" through its lens system. On some occasions, the capsule comes into direct contact with the intestinal wall, which can be seen pressed against the window in the front of the camera. In

healthy subjects after ingestion of the test meal, one third to one fourth of the images were blurred by the presence of turbid intestinal content. Detailed observation of endoluminal images suggests that intestinal content flow is compartmentalized so that fluid dynamics are quite segmental.

To test our hypothesis, we selected consecutive patients with clear-cut and severe symptoms suggestive of significant motor dysfunction of the small bowel; however, our patients were not in paralytic ileus or on total parenteral nutrition, ie, unable to feed by themselves. All underwent routine small bowel manometry using a standard technique. Patients with abnormal intestinal manometry were used as a training set, and, with this algorithm, the program recognized as abnormal part of the patients not fulfilling manometric criteria of dysmotility. The standard criteria used to diagnose small bowel motor dysfunction by manometry are very strict and were developed to detect abnormalities with high specificity.²⁰ The drawback is that only the most severe abnormalities are detected, and, hence, overall sensitivity is admittedly low. Furthermore, more prolonged recording time using 24-hour ambulatory manometry could potentially detect abnormalities, in particular during nighttime, missed by the 5-hour stationary technique we used.

Manometry exclusively provides information on the temporospatial organization of intestinal occlusive contractions that produce focal pressure peaks, but no information is collected the rest of the time. The functional significance of manometric patterns is limited, and only some events of content propulsion detected by fluoroscopy or impedance are associated with manometric pressure changes.^{21,22} In contrast to the multiple, punctual, and fixed recording sites of manometry, capsule endoscopy provides a 0.5-second image rate with a 1- to 3-cm depth of view obtained with a camera that moves within the gut. Overall, the findings in patients, eg, less contractile activity (luminal closure), more noncontractile patterns (open tunnel), more quiescence (static period), and more content retention (turbid images), fit well with the concept of motor impairment. Individual features permitted the identification of some patients, and the number of abnormalities provided a relatively good discriminative index. However, admitting that the functional significance of endoluminal image patterns is as uncertain as that of manometry, we adopted a black-box approach, letting the computer algorithm select the parameters that best discriminated patients from healthy subjects. Machine-learning techniques, which find the relative weight of combinations of features, offer significant advantages over single-feature discrimination. Furthermore, the specific algorithm used—in this case a support vector machine—also provides a numeric value related to the certainty of the diagnosis in both directions, ie, in subjects classified as normal or as abnormal. Ideally, the algorithm should have been developed in one group of

patients (training set) and validated in a second group. However, the complexity of the problem and the number of parameters analyzed call for a much larger sample size, not available for a single center pilot study. Hence, cross validation of the algorithm was performed by sequentially testing each subject using the remainder as the training set.

What is the potential relevance of this study? Conventional intestinal manometry is a complex technique that requires considerable expertise in its interpretation. This, in turn, can only be gained with routine performance of the test, and the critical numbers can only be achieved at specialized referral centers. The reality is that, currently, only a few centers around the world are capable of performing intestinal manometry on a routine basis. Under these circumstances, small bowel motor dysfunctions are currently underdiagnosed, which is an unfortunate situation. Evaluation of small bowel intestinal motility by capsule endoscopy is relatively noninvasive and simple to perform. Hence, our diagnostic method of motility dysfunction based on computer analysis of capsule studies could become available in virtually any gastrointestinal setting, both hospital and ambulatory, and the procedure can be repeated if technical problems, eg, the capsule not exiting the stomach, occur. The analysis of this technique is automated, does not require any experience, and is bias free. Furthermore, the capsule test, involving conventional endoscopy plus motility evaluation, provides a double set of complementary morphofunctional information on the small bowel. To date, our data support the applicability of this method in patients with severe, clear-cut motor dysfunction, and the present study shows it to be at least equal to intestinal manometry in yielding objective support to the purely clinical diagnosis. However, there remains much room for further improvement by expanding the training set, tuning the current algorithms for extraction and recognition of features, and introducing new features into the analysis program. These developments, and possibly also different testing conditions, may permit the diagnosis of more subtle motor abnormalities in patients with less specific clinical pictures.

References

1. Camilleri M, Hasler WL, Parkman HP, et al. Measurement of gastrointestinal motility in the GI laboratory. *Gastroenterology* 1998;115:747-762.
2. Frank JW, Sarr MG, Camilleri M. Use of gastroduodenal manometry to differentiate mechanical and functional intestinal obstruction: an analysis of clinical outcome. *Am J Gastroenterol* 1994;89:339-344.
3. Iddan G, Meron G, Glukhovskiy A, et al. Wireless capsule endoscopy. *Nature* 2000;405:417.
4. Stanghellini V, Camilleri M, Malagelada JR. Chronic idiopathic intestinal pseudo-obstruction: clinical and intestinal manometric findings. *Gut* 1987;28:5-12.
5. Wingate D, Hongo M, Kellow J, et al. Disorders of gastrointestinal motility: towards a new classification. *J Gastroenterol Hepatol* 2002;17(Suppl):S1-S14.
6. De Iorio F, Spyridonos P, Azpiroz F, et al. New insight into intestinal motor activity: correlation of endoluminal image analysis and displacement. *Gastroenterology* 2005;129:A24.
7. Vilariño F, Spyridonos P, Vitrià J, et al. A machine learning framework using SOMs: applications in the intestinal motility assessment. *Lect Notes Comput Sci* 2006;4225:188-197.
8. Kohonen T. *Self-organized maps*. Berlin: Springer, 1995.
9. Russ J. *The image processing handbook*. 5th ed. Boca Raton, FL: CRC Press, 2007.
10. Rubner Y, Tomasi C, Guibas LJ. The earth mover's distance as a metric for image retrieval. *Int J Comput Vis* 2000;40:99-121.
11. De Iorio F, Malagelada C, Azpiroz F, et al. In search for new parameters of intestinal motor activity in humans. *Gastroenterology* 2006;130:A473.
12. Rouillon J-M, Azpiroz F, Malagelada J-R. Sensorial and intestino-intestinal reflex pathways in the human jejunum. *Gastroenterology* 1991;101:1606-1612.
13. Serra J, Azpiroz F, Malagelada JR. Modulation of gut perception in humans by spatial summation phenomena. *J Physiol* 1998;506:579-587.
14. Vilariño F, Spyridonos P, Azpiroz F, et al. Cascade analysis for intestinal contraction detection. *Int J Comput Assist Radiol Surg* 2006;1:9-10.
15. Noble WS. What is a support vector machine? *Nat Biotechnol* 2006;24:1565-1567.
16. Spyridonos P, Vilariño F, Vitrià J, et al. Anisotropic feature extraction from endoluminal images for detection of intestinal contractions. *Lect Notes Comput Sci* 2006;4191:161-168.
17. Vilariño F, Spyridonos P, Vitrià J, et al. Linear radial patterns characterization for automatic detection of tonic intestinal contractions. *Lect Notes Comput Sci* 2006;4225:178-187.
18. Seguí S, Igual L, Radeva P, et al. A semi-supervised learning method for motility disease diagnostic. *Lect Notes Comput Sci* 2007;4756:773-782.
19. Stone M. Cross-validated choice and assessment of statistical predictions (with discussion). *J Roy Stat Soc B* 1974;36:111-147.
20. Stanghellini V, Cogliandro RF, De Giorgio R, et al. Natural history of chronic idiopathic intestinal pseudo-obstruction in adults: a single center study. *Clin Gastroenterol Hepatol* 2005;3:449-458.
21. Imam H, Sanmiguel C, Larive B, et al. Study of intestinal flow by combined videofluoroscopy, manometry, and multiple intraluminal impedance. *Am J Physiol Gastrointest Liver Physiol* 2004;286:G263-G270.
22. Rao SS, Lu C, Schulze-Delrieu K. Duodenum as an immediate brake to gastric outflow: a videofluoroscopic and manometric assessment. *Gastroenterology* 1996;110:740-747.

Received April 14, 2008. Accepted June 26, 2008.

Address requests for reprints to: Fernando Azpiroz, MD, Digestive System Research Unit, Hospital General Vall d'Hebron, 08035-Barcelona, Spain. e-mail: fernando.azpiroz@telefonica.net; fax: (34) 93 489 44 56.

Supported in part by Given Imaging, the Spanish Ministry of Education (Dirección General de Investigación, SAF 2006-03907), the Spanish Ministry of Health (Ayuda para contratos post-formación sanitaria especializada, CM05/00012), and the Instituto de Salud Carlos III (to Ciberehd).

The authors thank Maria Maluenda and Caterina Violanti for performing and visualizing the studies; Laura Igual, Panagiota Spyridonos Fernando Vilariño, and Jordi Vitrià for their contribution to the computer vision analysis program; Maite Casaus and Anna Aparici for technical support; Christine O'Hara for English editing of the manuscript; and Gloria Santaliesra for secretarial assistance.

Financial disclosure and conflicts of interest: Supported in part by Given Imaging. No conflicts of interest exist.